

# The weldability of AISI 4340-AISI 2205 steels using friction welding

U. CALIGULU\*, M. YALCINOZ<sup>a</sup>

*Firat University, Faculty of Technology, Dept. of Met. and Materials Eng., Elazig, Turkey*

<sup>a</sup>*Firat University, Faculty of Technical Education, Dept. of Metallurgy Education, Elazig, Turkey*

---

In this study, the weldability of AISI 4340-AISI 2205 steels using friction welding was investigated. AISI 4340 tempered steel and AISI 2205 duplex stainless steel each of which had a 12 mm diameter were used to fabricate the joints. The friction welding tests were performed by using a direct-drive type friction welding machine. After friction welding, interface regions of the welded specimens were examined by OM, SEM, EDS and X-Ray analysis to determine the microstructure changes. Microhardness and tensile tests were conducted to determine mechanical properties of the welded specimens. The experimental results indicated that AISI 4340 tempered steel could be joined to AISI 2205 duplex stainless steel using the friction welding technique for achieving a weld with sufficient strength. Tensile strength values also confirmed this result and intermetallic phases did not occur at the interface. The maximum tensile strength of 624.89 MPa could be obtained for the joints welded under the welding conditions as follows; of rotation speed of 2200 rpm, friction pressure of 30 MPa, forging pressure of 60 MPa, friction time of 6 s and forging time of 3 s.

(Received November 19, 2014; accepted June 24, 2015)

**Keywords:** AISI 4340, AISI 2205, Friction Welding, Microstructure, Tensile Strength

---

## 1. Introduction

In recent years, the consumer industry has been incorporating a variety of materials in its products made on a large scale to improve the performance and reduce the costs. This has resulted in increased demands for techniques to weld dissimilar materials and for use in large scale industrial production. Friction welding can be used to join metals of widely differing thermal and mechanical properties [1-2-3].

Friction welding is a solid state joining process which can be used to join a number of different metals. The process involves making welds in which one component is moved relative to, and in pressure contact, with the mating component to produce heat at the faying surfaces. Softened material begins to extrude in response to the applied pressure, which create an annular upset. Heat is conducted away from the interfacial area for forging. The weld is completed by applying a forge force during or after the cessation of relative motion. The joint undergoes hot working to perform a homogenous, full surface, and high-integrity weld [4-8]. Friction welding is the only viable method in this field to overcome the difficulties encountered in the joining of dissimilar materials with a wide variety of physical characteristics. Compared to others, the advantages of this process are; no melting, high reproducibility, short production time and low energy input [9-13].

Tempered types of steel are machinery manufactured steels with and without alloy, whose chemical compositions, especially in terms of carbon content, are suitable for hardening and which shows high toughness under a specific tensile strength at the end of the tempering process. Tempered types of steel, due to their superior

mechanical properties, acquired at the end of the tempering process, are used in a wide range including the manufacture of parts such as various machine and engine parts, forging parts, various screws, nuts and stud bolts, crank shafts, shafts, control and drive components, piston rods, various shafts, gears. For this reason, tempered steels are the type of steel used and produced at the highest rate after the unalloyed steels and construction steels. These steels constitute the most important part of the machinery-manufacturing steels. Generally, such steels are used for the production of fitting, axle shaft, the shaft and the gear [14-18].

Stainless steels are popularly used in industries because of its corrosion resistance. Types of steels can be identified based on the microstructure and major crystal phase. Duplex stainless steel (DSS) is the mixture of austenitic and ferritic stainless steel. Hence, it has inherent properties such as high fatigue strength, good pitting resistance and weldability, high mechanical strength and good in corrosion resistance due to high content of chromium. 2205 DSS is widely employed in desalination plants, pulp industry, bridges, pressure vessels cargo tanks, pipe system in chemical tankers, and heat exchangers due to both excellent corrosion resistance and high strength [19-20]. Urena [21] developed the optimum welding condition for joining 2205 DSS using plasma-arc welding. Ku et al [22] welded 2205 duplex stainless steel by electron beam welding and analyzed the mechanical properties, microstructure and corrosion properties of the weldment. Kannan and Murugan [23] observed the effects of FCAW process parameters on DSS clad quality. Laser beam welding parameters were optimized by Reisgen et al [24] and they found that, RSM can be considered as a powerful tool in experimental welding optimization. As

the weld bead quality depends on the process parameters, it is essential to study the effects of process parameters on weld quality.

Dobrovidov [25] investigated the selection of optimum conditions for the friction welding of high speed steel to carbon steel. Ishibashi et al [26] chose stainless steel and high speed steel as representative materials with an appreciably difficult weldability, and their adequate welding conditions were established. The distributions of the alloying elements at and near the weld interface with sufficient strength were analyzed by using X-ray microanalysis, Mumin Sahin [15] analyzed the variations in hardness and microstructure at the interfaces of friction welded steel joints. While using austenitic stainless steel, negative metallurgical changes like delta ferrite formation and chromium carbide precipitation between grain boundaries took place during fusion welding. These changes were eliminated by friction welding. The effect of friction time on the fully plastically deformed region in the vicinity of the weld was investigated by Sathiya et al [27]. Ananthapadmanaban et al [28] reported the effect of friction welding parameters on tensile properties of steel. Satyanarayana et al [29] joined austenitic- ferritic stainless steel (AISI 304 and AISI 430) by using continuous drive friction welding and investigated optimum parameters, microstructures-mechanical properties and fracture behaviors. Yilmaz [30] investigated the variations in hardness and microstructures in the welding zone of friction welded dissimilar materials. The effect of friction pressure on the properties of hot-rolled iron-based superalloy was investigated by Ates et al [31]. Meshram et al [32] investigated the influence of interaction time on microstructure and tensile properties of the friction welding of dissimilar metal combinations. Paventhan et al

[33] examined optimization of friction welding process parameters for joining carbon steel and stainless steel.

In this study, the objective of the present work is to examine the weldability of AISI 4340-AISI 2205 steels using friction welding were investigated.

## 2. Experimental procedures

AISI 4340 tempered steel and AISI 2205 duplex stainless steel of 12 mm diameter were used to fabricate the joints in this study. Table 1 illustrates the chemical compositions of the base metals. The friction welding tests were carried out using a direct-drive type friction welding machine. While Table 2 present mechanical properties of AISI 4340 and AISI 2205 Table 3 shows physical properties of AISI 4340 and AISI 2205 steels. Table 4 illustrates the experimental conditions. The experimental set-up is shown in Fig. 1.

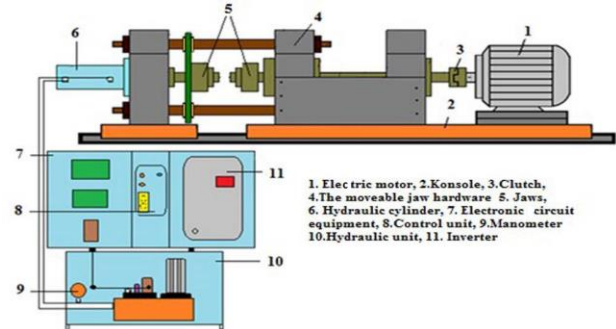


Fig. 1. Experimental set-up [7].

Table 1. Chemical compositions of test materials.

Materials	Alloy Elements (% wt)									
	C	Mn	Si	P	S	Cr	Mo	Ni	N	Cu
AISI 4340	0.4	0.8	0.3	0.035	0.040	0.9	0.3	2.00	-	-
AISI 2205	0.018	1.686	0.309	0.026	0.003	22.333	3.379	4.932	0.191	0.097

Table 2. Mechanical properties of copper and low carbon steel.

Materials	Tensile Strength (MPa)	Yield Strength 0.2% (MPa)	Elongation (%)	Microhardness (HV)
AISI 4340	659	400	20.98	201
AISI 2205	956	620	20	328

Table 3. Physical properties of copper and low carbon steel.

Materials	$\alpha$ $10^{-6}$	$\lambda$ W/m °C	$\Omega$ n $\Omega$ m	E GPa
AISI 4340	12.3	44.5	248	190-200
AISI 2205	14.7	19	85	200
$\alpha$ : Thermal Expansion Coefficient (20-800 °C)		$\lambda$ : Thermal Conductive (20 °C)		
$\Omega$ : Electrical Resistance (20 °C)		E: Elastic modulus (20 °C)		

After friction welding procedure, specimens were divided into sections transversely in order to investigate the micro-structural variations from the centre to the outside of the weld. Transverse sections were prepared, and then grinding and polishing processes of 3  $\mu\text{m}$  diamond paste were performed in order to conduct metallographic examination of the joined materials. The specimens were etched in a solution 2%  $\text{HNO}_3$  + 98% alcohol for tempered steel and in a solution 25%  $\text{HNO}_3$  +

75% pure water for duplex stainless steel to conduct the micro-structural examination (7.5 Volt + 30 sec.) The microstructures of the joints were observed by using Optical Microscopy (OM), the Energy Dispersive Spectroscopy (EDS) and X-Ray Diffraction (XRD). Micro-hardness measurements were taken under a load of 50 g. Tensile tests were conducted at room temperature with  $10^{-2} \text{ mm s}^{-1}$  cross-head rate.

Table 4. The process parameters used in the friction welding.

Sample no	Welding parameters					
	Rotating speed(rpm)	Friction pressure(MPa)	Forging pressure(MPa)	Friction time(S)	Forging time(s)	Axial shortening(mm)
S1	2200	30	60	6	3	4.00
S2	2200	30	60	10	5	4.37
S3	2100	30	60	6	3	3.15
S4	2100	30	60	10	5	3.41
S5	2000	30	60	6	3	2.10
S6	2000	30	60	10	5	2.80

### 3. Results and discussion

#### 3.1 Evaluation of microstructures

The macro-view of specimens S1, S2, S3, S4, S5 and S6 welded under different welding conditions is shown in Fig. 2. Visual examination of the welded specimens showed uniform weld joints. As is seen in Fig. 2, the amount of flash increased with an increase in friction time, forging time, and rotation speed. In the case that the dissimilar materials are joined by using the friction welding method, the formation of the flash depends on the mechanical properties of two parent materials. Maximum post-welding axial shortening is was measured as 4.37 mm on specimen S2.



Fig. 2. Overview of friction welded AISI 4340-AISI 2205 steels.

The flash obtained was symmetric, which indicated plastic deformation on both the rotating and upsetting (reciprocating) side. The integrity of the joints was evaluated for the friction-welded joints. The friction processed joints were sectioned perpendicular to the bond line and observed through an OM microscope. It can be

clearly seen that, there were no crack and voids at the weld interface. According to the microstructural observations, the microstructures formed interface zone during or after FW processes, and there were three distinct zones across the specimens as unaffected zone (UZ), deformed zone (DZ) and transformed and recrystallized fully plastic deformed zone (FPDZ). Typical grain refinement occurred in the DZ region by the combined effect of thermal and mechanical stresses (Fig. 3). A typical micrograph showing the different morphologies of the microstructure at different zones of the friction processed joint is shown in Fig. 3.

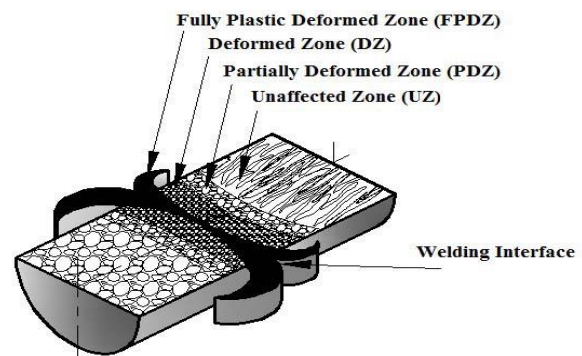


Fig. 3. Regions which occurred microstructural changes [34].

It was observed that the rotational speed had an effect on geometry and width of the weld zone. The mechanical deformation and the frictional heat at the interface that diffused through the parent materials resulted in an increase in temperature gradient, which caused different zones in the microstructure. Although this condition

caused lower cooling rates and a wider (HAZ), higher rotation speed lead narrower FPDZ due to a greater volume of viscous material transferred out of the interface. It is a known fact that when pressure is used to bring joint pair together by plastic deformation, this results in dynamic recrystallization leading to a grain refinement in the central region of the weld. The effect of increasing rotation speed on the friction welded joint was an increase in both temperature gradient and axial shortening as a result of more mass being transferred out of the welding interface. High rotation speed could cause local heating at

the interface, thus reaching a high temperature in a short time. This condition caused lower cooling rates and a wider heat affected zone (HAZ), as a consequence of a greater volume of viscous material transferred out of the interface. AISI 4340 tempered steel was greatly deformed by the severe plastic deformation and frictional heat near the weld zone. There were no blanks, cracks or porosities in the weld zone (Fig. 4).

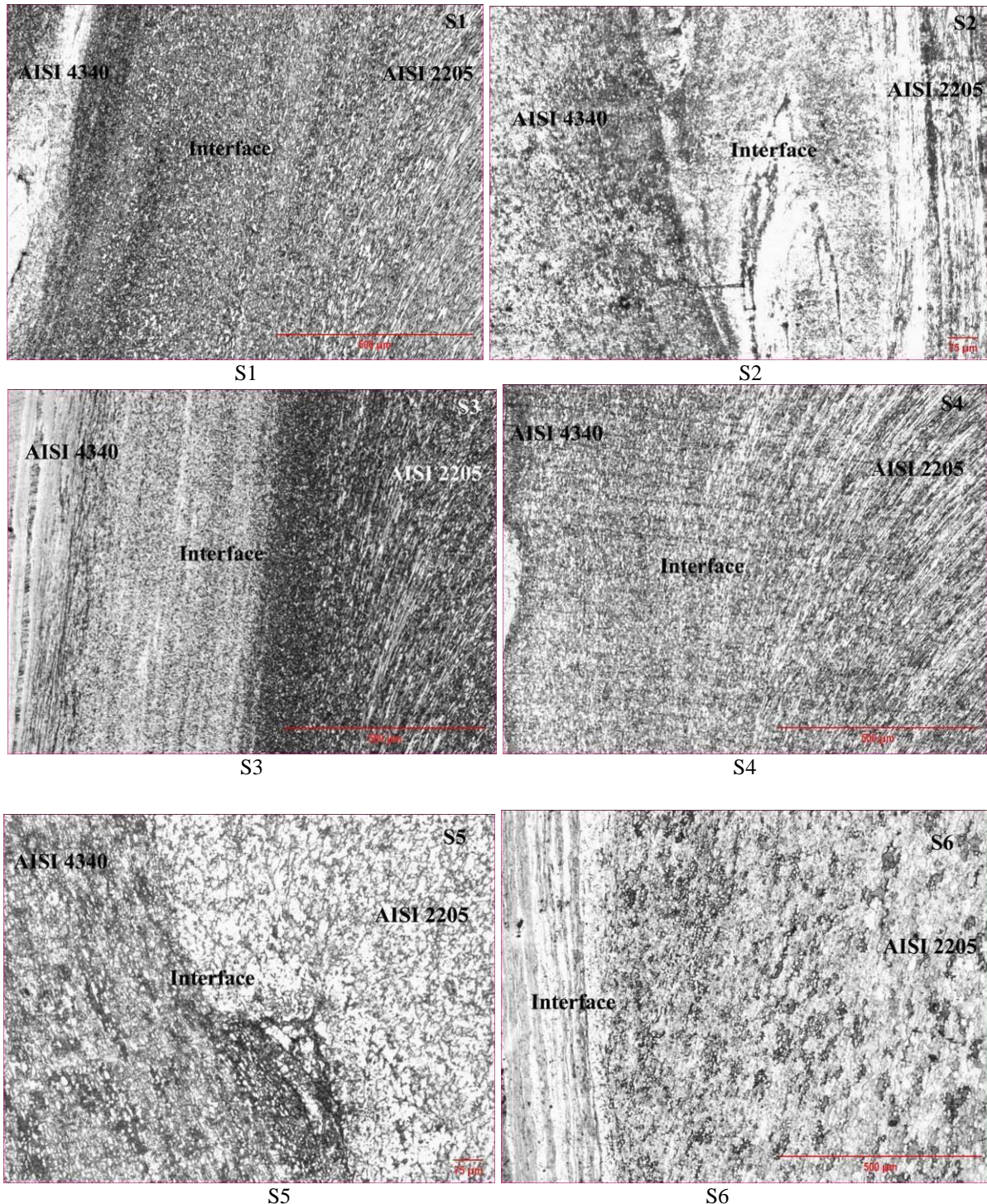


Fig. 4. Optical micrograph taken from the welding interface of the specimens S1, S2, S3, S4 S5 and S6 respectively.

During the friction welding process, the temperature at the interface was measured by using IGA 15 PLUS detector and the temperature values at the interface of the joints are given in Fig. 5. It shows that the temperature observed at the interface of the joint was lower than to melting temperature of AISI 4340 tempered steel (1034–1180 °C).

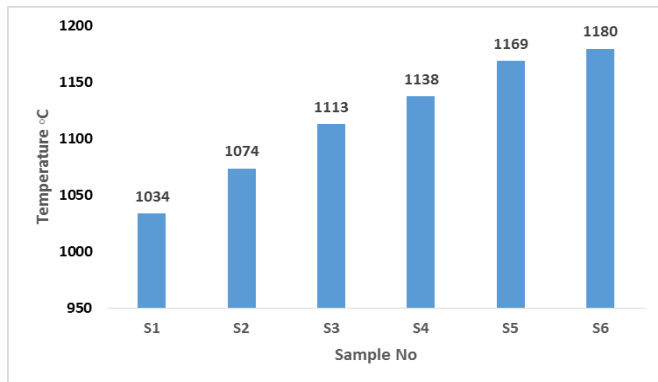


Fig. 5. The temperature at the interface of FW joints during welding.

### 3.2. Tensile test results

Shape and measurements of the tensile specimens are present in Figure 6. The results of tensile tests are present in Figs. 7 and 8, respectively. As is clearly seen in Fig. 8, the tensile strength slightly increased while the rotation speed increased. Results of the tensile tests concluded that all joints were fractured by necking at the tempered steel side (see Fig.7). Current studies in literature have reported that a higher bonding temperature results in profuse inter-diffusion and better coalescence of mating surfaces. Plastic deformation detected in the specimens after the welding was not observed. However, increasing bonding temperature due to the increase of the rotation speed and the friction time also promoted the growth of brittle intermetallic, which adversely affected the bond strength in turn. Therefore, low elongation and strength values can be attributed to presence of aligned tempered steel precipitation reducing these properties. Maximum tensile strength and minimum temperature of the FW joints were, 624.89 MPa and 1034 °C, respectively at 2200 rpm in S1. This increase in tensile strength was related to the heat input and high plastic deformation occurring at the component interface as a result of the rotational speed and the axial pressure. Minimum tensile strength and maximum temperature of FW joints were 598.24 Mpa and 1180 °C, respectively at 2000 rpm in S6. This decrease in tensile strength was associated with the reactions taking place at HAZs of the tempered steel side. Longer time intervals allowed the thermal energy to propagate along the axial direction of the work materials, and as a consequence, a bulk volume of material was heated. Therefore, longer time intervals led to lower cooling rates and a wider HAZ. As the friction time decreased, the

joining efficiency steeply increased, and reached a maximum value at 2200 rpm for 6 s with 624.89 MPa and then decreased again. Under given conditions (2200, 2100 and 2000 rpm rotation speeds) tensile strengths were close to parent material, and slightly increased with increased rotation speeds.

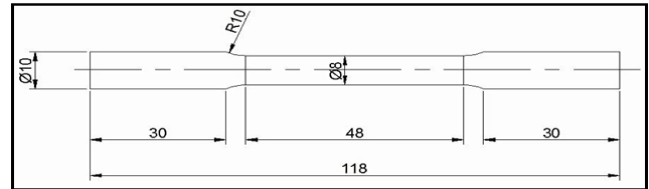


Fig. 6. Shape and measurement of the tensile test specimens [TSE 138] [35].



Fig. 7. Optical macro-photo of tensile test results of friction-welded joints.

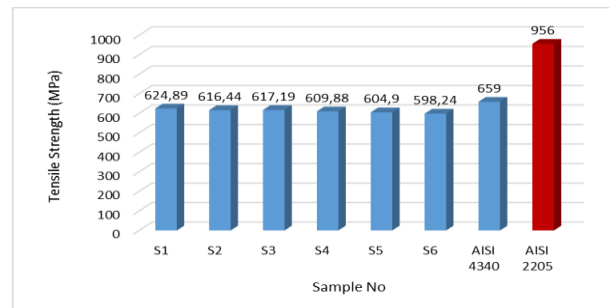


Fig. 8. Tensile test results of friction-welded joints.

### 3.3. Fractography

Fig. 9 shows the images of the fracture surfaces caused by the tensile test for the friction-welded specimens S1 and S6. Examining the fracture surface images, fractures caused by the tensile test were mostly on the AISI 4340 tempered steel side, and it was observed that the fracture surface contained ductile dimples, formed by the microvoid coalescence mechanism and facets associated with the cleavage fracture. The dimples were believed to initiate at the second-phase particles or small

inclusions within the ferrite and austenite phase of the AISI 2205 duplex stainless steel; whereas the facets represent brittle fracture occurring along the cleavage planes of the phase. As illustrated in Fig. 9, the number of ductile

dimples increased with decreasing rotation speed. This type of fracture topography is classified as the quasi-cleavage. In generally, mechanism of ductile fracture was observed in the specimens.

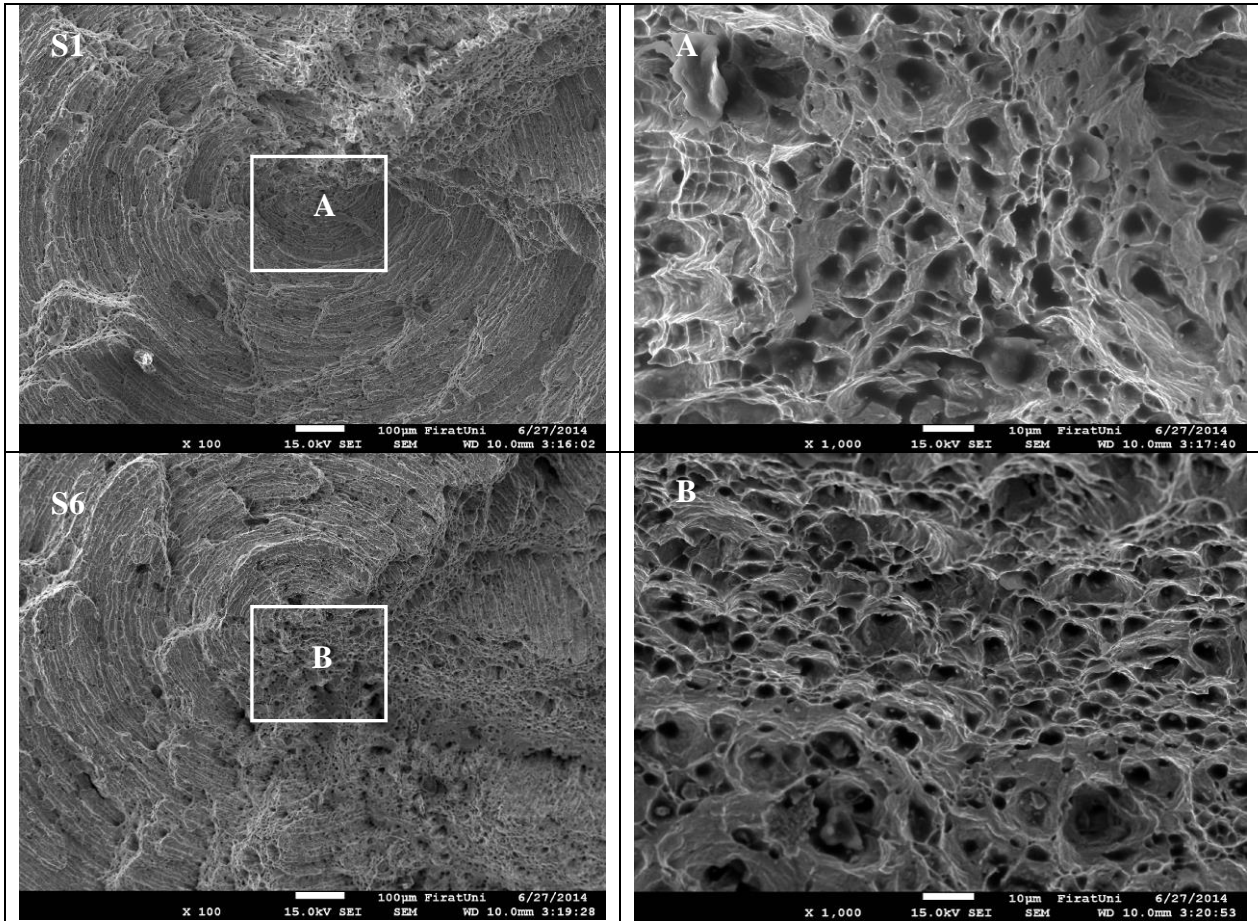


Fig. 9. Micrograph of the tensile fracture surfaces of S1 and S6 specimens observed by SEM.

### 3.4. Microhardness

Fig. 10 illustrates microhardness measurements in the direction perpendicular to the weld interface of the friction-welded joints for specimens S1–S6. As seen in this figure, a significantly similar trend was observed in the microhardness profiles of all specimens. The increasing hardness in the welding interface can be directly associated with the microstructure in the welding interface, as a result of the increasing heat input and severe plastic deformation. Microhardness values could increase with increasing rotation speed and friction time. Relatively higher hardness could be explained with the C, Cr, Mn, Fe and Ni diffusion of parent materials at the weld interface. The increase in hardness in the AISI 4340 side could be attributed to the work hardening of the duplex stainless steel. Besides, the main reason for this was associated with the temperature increase in the interface, which was caused by deformation and friction. The temperature increase caused by the increase in the friction time enhanced the viscosity of the material in the interface and enabled it to remove out of the interface quickly. The

increase in the upset time, on the other hand, was thought to create a forging effect on AISI 4340 side and cause an increase in hardness.

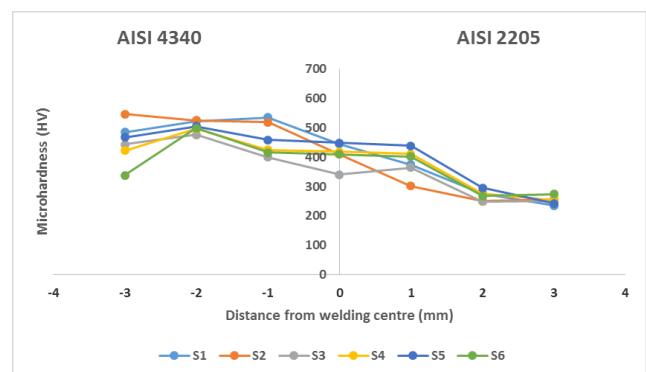


Fig. 10. Microhardness distribution across the welding interface of friction-welded specimens.

### 3.5. X-Ray diffraction and EDS analysis

Fig. 11 illustrates X-Ray diffraction across the interface of the specimen S1. In the X-Ray analysis, like Fe-Ni, Fe-Cr-Ni, Fe-Cr,  $Cr_{23}C_6$ , Cr-Fe-Ni-C and  $Cr_7C_3$  phases were determined (Fig. 11). In the EDS analysis, as well as C, Cr, Mn, Fe and Ni elements, no intermetallic phases were determined at the welding interface. In 60  $\mu m$  distance, duplex stainless steel Fe, C and Mn diffusion occurred from AISI 4340 tempered steel, and also Cr and Ni diffusion occurred from AISI 2205 steel to AISI 4340 at equal distance (Table 5 and Fig. 12). The frictional heat generated at the interface (under identical welding conditions) would be high for low-density elements due to their high boundary friction coefficients and low thermal conductivity compared to high density elements. The welding procedure made with dissimilar materials exhibited wider plasticized zone in the center of the welding interface. As for low-density elements, intermixing elements were larger in comparison to high-density elements. This was due to the fact that higher flow required for the high-density elements restricted movement compared to the low-density elements which can move freely.

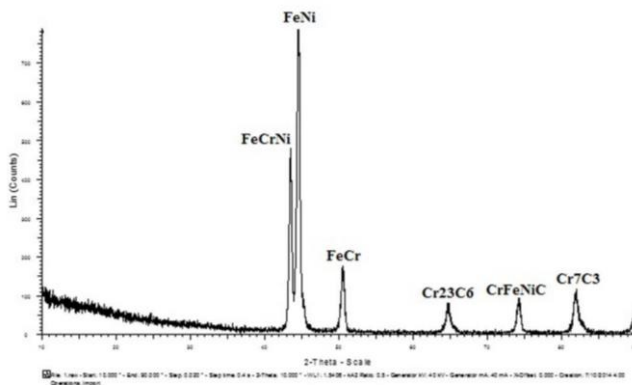


Fig. 11. The result of XRD analyses S1 specimen.

Table 5. Quantity of concentration taken from EDS analysis across the welding interface of S1 specimen.

EDS point	Alloying elements (wt%)				
	C	Cr	Mn	Fe	Ni
1	13,34	0,88	1,29	83,35	1,13
2	11,85	8,71	2,02	75,71	1,71
3	10,94	15,44	1,99	67,96	3,66

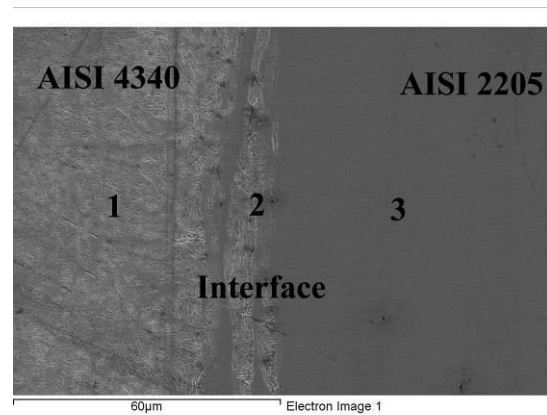
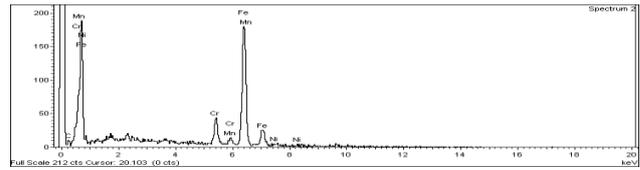


Fig. 12. EDS analyses across the welding interface of the friction-welded specimen S1.

### 4. Conclusion

AISI 4340 tempered steel and AISI 2205 duplex stainless steel were joined by friction technique using different process parameters. Below are conclusions drawn based on the results of microstructure analysis, hardness and tensile tests.

1. This study concluded that AISI 4340 tempered steel could be joined successfully to AISI 2205 duplex stainless steel by using the friction welding technique. Comprehensive micro-structural investigations for friction welded AISI 4340/2205 revealed that there were different zones at the welding interface, the wideness of fully plasticized deformed zone (FPDZ) decreased when rotation speed and forging time increased.
2. The higher microstructural changes took place in HAZs. An increase in the contraction of the samples was observed after increasing friction welding rotation speeds. The width of HAZ is mainly affected by friction time and rotation speed. This signifies that the width and formation of HAZs which occurred as a result of the reactions taking place at the welding interface had an adverse effect on the mechanical strength and consequently, the quality of the friction-welded joints.
3. The highest deformation was always observed at AISI 4340 side and in all specimens the original structure was preserved in the undeformed zone.
4. A rotation speed of 2000 rpm was not completely sufficient for joining AISI 4340/2205 steels by friction welding, but a rotation speed of 2200 rpm was sufficient for joining these materials.
5. The maximum tensile strength of 624.89 MPa could be obtained for the joints welded under the welding conditions as rotation speed of 2200 rpm, friction

pressure of 30 MPa, forging pressure of 60 MPa, friction time of 6 s and forging time of 3 s.

6. All specimens were subjected to tensile testing and brittle characteristics of the fracture topography were observed in the partially deformed zone on AISI 4340 steel side.
7. The increase in hardness at HAZs is attributed to the micro-structural transformation that occurred during the friction welding process. The strengthening effect observed in this zone was mostly a direct result of the rapid cooling from the welding temperature. For achieving a welding with sufficient strength, the friction time has to be held as short as possible, whereas the rotation speed has to be as high as possible.
8. In X-Ray analysis, Fe-Ni, Fe-Cr-Ni, Fe-Cr, Cr<sub>23</sub>C<sub>6</sub>, Cr-Fe-Ni-C and Cr<sub>7</sub>C<sub>3</sub> phases were determined. In the EDS analysis, as well as C, Cr, Mn, Fe and Ni elements, no intermetallic phases were determined in the welding interface. In 60 μm distance, duplex stainless steel Fe, C and Mn diffusion occurred from AISI 4340 tempered steel, and also Cr and Ni diffusion occurred from AISI 2205 steel to AISI 4340 at equal distance.

## References

- [1] I. Kirik, N. Ozdemir, *International Journal of Materials Research*, **104**(8), 769 (2013).
- [2] N. Ozdemir, F. Sarsilmaz, A. Hascalik, *Mater. Des.*, **28**, 301 (2007).
- [3] *Welding handbook*, Welding Processes, Volume 2, Eighth edition. Copyright by the American Welding Society Inc., Miamis, 739 (1997).
- [4] R. E. Chalmers, *Manufacturing Engineering*, **126**, 64 (2001).
- [5] N. Ozdemir, *Materials letters*, **55**, 2504 (2005).
- [6] D. E. Spindler, *Welding Journal*, 37 (1994).
- [7] I. Kirik, N. Ozdemir, U. Caligulu, *Kovove Materials*, **51**(4), 221 (2013).
- [8] P. Sathiya, S. Aravindan, A. Noorul Haq, *Materials and Design*, **29**, 1099 (2007).
- [9] I. Kirik, N. Ozdemir, F. Sarsilmaz, *MP Material Testing*, **54**(10), 683 (2012).
- [10] M. B. Uday, M. N. Ahmad Fauzi, H. Zuhailawati, A. B. Ismail, *Science and Technology of Welding and Joining*, **15** (7), 534 (2010).
- [11] J. Domblesky, F. F. Kraft, *Journal of Materials Processing Technology*, **191**, 82 (2007).
- [12] S. Celik, I. Ersozlu, *Materials and Design*, **30**, 970 (2009).
- [13] S. Celik, D. Dinc, R. Yaman, I. Ay, *Practical Metallography*, **47**(4), 188 (2010).
- [14] S. D. Meshram, T. Mohandas, G. Madhusudhan Reddy, *Journal of Materials Processing Technology*, **184**, 330 (2008).
- [15] P. Sathiya, S. Aravindan, A. Noorul Haq, *Materials and Design*, **29**, 1099 (2008).
- [16] S. Celik, I. Ersozlu, *Mater. Des.*, **30**, 970 (2009).
- [17] <http://www.celmercelik.com>.
- [18] M. Sahin, H. E. Akata, *Indust. Lubricat. Tribol.*, **56**, 122 (2004).
- [19] G. B. Rajkumar, N. Murugan, *Indian Journal of Engineering & Materials Science*, **21**, 149 (2014).
- [20] Y. S. Kim, T. W. Eagar, *Welding Journal*, **72**(7), 279 (1993).
- [21] A. Urena, *Journal of Materials Processing Technology*, *Journal of Materials Processing Technology*, **182**, 624 (2007).
- [22] J. S. Ku, N. G. Ho, S. C. Tjong, *Journal of Materials Processing Technology*, **63**, 770 (1997).
- [23] T. Kannan, N. Murugan, *Journal of Materials Processing Technology*, **176**, 230 (2006).
- [24] U. Reisgen, M. Schleser, O. Mokrov, E. Ahmed, *Optic Laser Technology*, **44**, 255 (2012).
- [25] A. N. Dobrovidov, *Weld Prod*, **22**(3), 226 (1975).
- [26] A. Ishibashi, S. Ezo, S. Tanaka, *Bulletin of The JSME*, **26**(216), 1080 (1983).
- [27] P. Sathiya, S. Aravindan, A. Noorul Haq, *Int J Adv Manuf Technol*, **26**(5/6), 505 (2005).
- [28] D. Ananthapadmanaban, V. Seshagiri Rao, Abraham Nikhil, *Materials and Design*, **30**(7), 2642 (2009).
- [29] V. V. Satyanarayana, G. Madhusudhan Reddy, T. Mohandas, *Journal of Materials Processing Technology*, **160**(2), 128 (2005).
- [30] M. Yilmaz, Technical University of Yildiz, 1993.
- [31] H. Ates, M. Turker, A. Kurt, *Materials and Design*, **28**(3), 948 (2007).
- [32] S. D. Meshram, T. Mohandas, G. Madhusudhan Reddy, N. Journal of Material Processing Technology, **1840**(2/3), 330 (2007).
- [33] R. Paventhan, P. R. Lakshminarayanan, V. Balasubramanian, *Journal of Iron and Steel Research International*, **19**(1), 66 (2012).
- [34] S. Mercan, N. Ozdemir, *NWSA-Technological Applied Sciences*, 2A0080, **8**(2), 18 (2013).
- [35] N. Kati, S. Ozan, *NWSA (New World Science Academy)*, 2A0086, 22 (2014).

\*Corresponding author: ucaligulu@firat.edu.tr